CrystEngComm

Accepted Manuscript

ROYAL SOCIETY OF CHEMISTRY

www.rsc.org/crystengcomm

Salt-assisted Rapid Transformation of $NaYF_4$: Yb^{3+},Er^{3+} Nanocrystals from Cubic to Hexagonal

Bangda Yin, Wenli Zhou, Qian Long, Chengzhi Li, Youyu Zhang*, Shouzhuo Yao

Key Laboratory of Chemical Biology and Traditional Chinese Medicine Research (Ministry of Education, College of Chemistry and Chemical Engineering, Hunan Normal University, Changsha 410081, China

Abstract:

High-quality hexagonal upconversion nanocrystals of β-$NaYF_4$:Yb^{3+},Er^{3+} were prepared through one-pot mild solvothermal synthesis. The crystal structure of $NaYF_4$:Yb^{3+},Er^{3+} can rapid transform from cubic (α-) to β- phase in the presence of some salts, such as sodium hydrogen phosphate (Na_2HPO_4). It was found that the size and structure of as-prepared $NaYF_4$:Yb^{3+},Er^{3+} can be controlled by changing the molar ratio of phosphate to Ln^{3+} (Ln^{3+} represents the total amount of Y^{3+} and the doped rare earth elements such as Yb^{3+}, Er^{3+}). The possible formation mechanism was proposed on the basis of XRD analysis and TEM observation of the products at the different reaction condition. The upconversion fluorescence at 550 nm of β-$NaYF_4$:Yb^{3+},Er^{3+} nanocrystals with spherical structure and narrow size distribution was enhanced up to 22.5-fold compared to cubic nanocrystals (α-$NaYF_4$:Yb^{3+},Er^{3+}). This study also is expected to be provided a reference for exploration of other complex with controllable structure and optical properties.

* Corresponding author: Tel: +86-731-8865515; fax: +86-731-8865515;
Email address: zhangyy@ hunnu.edu.cn

1 Introduction

The nano- and micro-structure materials have attracted considerable attention due to their potential applications in various fields during the past decades.[1-5] The chemical and physical properties of the materials are related to their morphologies, sizes and crystal structure.[6, 7] Therefore, many works have been done surrounding the research about the physical mechanism and the method for controlling the crystallization processes for obtains the desired shape of crystals.[7, 8] Some theoretical models also have been introduced to explain the relationship between equilibrium morphology and crystal structure.[6, 8] However, it is still a challenge to develop a facile approach to manipulate and control the morphologies and crystal phase of various inorganic crystals owing to the complexity of crystal structures and compositions of these materials.[9] Therefore, the synthetic method with no expensive reagents and complex equipments for controlling the morphologies and structure of crystals is attracting great interest. Some additives, such as polyvinyl pyrrolidone (PVP)[6], ethylene diamine tetraacetic acid (EDTA)[10], ethanediamine[11], sodium citrate and AOT[12], can be used to control the phase, morphology, and size of crystal materials. Ongoing efforts have been performed to examine the surface energies of crystals in the presence and absence of additives in order to confirm the role of these additives to structured materials.[13, 14] Some salts

were also used as the additive to control the morphology and structure of some crystals.[15-18] However, the action of surfactants for controlling the phase, morphology of crystals is still not perfect.[6]

Among these crystal materials, upconversion nanocrystals (UCNCs) with the advantages of no background fluorescence, perfect tissue penetration and low toxicity have been applied in the fields of bioanalysis, disease diagnosis, optical communication and solar cells.[19-21] As one of host matrixes, sodium yttrium fluoride ($NaYF_4$) with low phonon energies (<400 cm^{-1})[12] and a high refractive index (1.430-1.470 m^2/W) has been considered as an excellent host matrix for down-conversion (DC) and up-conversion (UC) nanocrystals synthesis[12]. The ytterbium and erbium co-doped sodium yttrium fluoride ($NaYF_4:Yb^{3+},Er^{3+}$) nanocrystals is one of the most efficient upconversion fluorophores among various kinds of upconversion materials[5] and cubic (α-) and hexagonal (β-) phases are the two polymorphic forms for it. It is known that the β- $NaYF_4:Yb^{3+},Er^{3+}$ crystals exhibits considerable higher fluorescence efficiency than that of α-$NaYF_4:Yb^{3+},Er^{3+}$ crystals.[7, 12] Thermal decomposition method was used for the synthesis of $NaYF_4:Yb^{3+},Er^{3+}$ nanocrystals frequently.[22-24] High-quality UCNCs can be successfully produced from the metal trifluoroacetate precursors ($(CF_3COO)_3Ln$) in the presence of high boiling point organic solvents.[23] However, the generation of toxic by-products, expensive and air-sensitive metal precursors and rigorous synthesis

conditions limited its operability[25]. The hydro/solvothermal method with the simple operations (one-pot synthesis) was also used for preparing inorganic submicrocrystalline materials.[10, 26] However, long hydrothermal time (>10 h) and a higher temperature (>200 ^{o}C) are needed to synthesize the phosphors with β- phase (β-$NaYF_4$:Yb^{3+},Er^{3+}).[7] Many methods have been used to control morphology and phase of crystal. Wu reported the hydrothermal growth of β-$NaYF_4$ by altering the hydrothermal reaction temperature and the reaction time.[27] Solvothermal conditions were employed to fabricate different microstructures of β-$NaYF_4$:Yb^{3+},Er^{3+} [28] and $NaYF_4$.[29] By adjusting solvent composition and F^-/Ln^{3+} molar ratio can fabricate β-$NaYF_4$:Yb^{3+},Er^{3+} nanocrystals at 240 ^{o}C by using a facile hydrothermal method.[7] However, spherical nanocrystals with small size and high-efficiency fluorescent are preferred for biological applications, it is still a challenge to fabricate well-defined $NaYF_4$ crystals with the ideal size, morphology and crystal phase.[9] To the best of our knowledge, there is no report on using inorganic salts to control the morphologies and crystal structure of UCNCs in reaction process.

In this paper, we report a facile hydrothermal approach for the fabrication β-$NaYF_4$:Yb^{3+},Er^{3+} nanocrystals with well-defined morphology by assist of Na_2HPO_4 which can regulate the nucleation and growth behaviour of the crystals with considerably mild conditions and shortened time. More specifically, the other inorganic salts, such as NaCl,

Na_2SO_4, $(NH_4)_2HPO_4$, with different degrees, can also promote the rapid transformation of the crystal from α- phase (α-$NaYF_4$:Yb^{3+},Er^{3+}) to high-quality β-$NaYF_4$:Yb^{3+},Er^{3+} crystals. The morphologies and sizes can be controlled by simply tuning the molar ratio of phosphate to Ln^{3+} and the possible formation mechanism for the phase evolution process of $NaYF_4$:Yb^{3+},Er^{3+} is also presented. Furthermore, the upconversion fluorescence properties of $NaYF_4$:Yb^{3+},Er^{3+} were also investigated. This method for UCNCs with controllable phase is expected to expand in exploration of other inorganic crystals complex.

2 Experimental

2.1 Apparatus

The crystal phase of the products was identified by a Rigaku 2500 (Japan) X-Ray Diffractometer (XRD) with 2θ range from 10° to 70° at a scanning rate of 4° per minute, with Cu Ka irradiation (k=1.5406 Å). The size and morphology of the transmission electron microscopy (TEM) images were characterized using a JEOL-1230 TEM (JEOL, Japan). The fluorescence spectra were measured using an F-4500 fluorescence spectrophotometer (Hitachi Ltd, Japan) with an external 980 nm laser diode (Hi-Tech Optoelectronic Co., Ltd. China) as the excitation source. All samples were prepared using ultrapure water obtained from a Mill-Q water purification system (Millipore, ≥18 MΩ cm).

2.2 Materials

Rare-earth oxides used in this work, including yttrium oxide (Y_2O_3), ytterbium oxide (Yb_2O_3) and erbium oxide (Er_2O_3), were purchased from Sinopharm Chemical Reagent Co., Ltd. (Shanghai, China) and dissolved in hot nitric acid and then dissolved in deionized water to achieve final concentrations of 0.4 M, 0.05 M, and 0.05 M, respectively. Sodium phosphate dibasic dodecahydrate ($Na_2HPO_4 \cdot 12H_2O$), hydrofluoric acid (HF), sodium hydroxide (NaOH), nitric acid (HNO_3), cetyltrimethyl

ammonium bromide (CTAB) and EDTA were of analytical grade from Sinopharm Chemical Reagent Co., Ltd. (Shanghai, China) and were used as received without further purification.

2.3 The synthesis of $NaYF_4$: Yb^{3+},Er^{3+}

The UCNCs were prepared according to a modified synthesis procedure[10], 1.315 mL of 0.4 M $Y(NO_3)_3$, 0.42 mL of 0.05 M $Yb(NO_3)_3$ and 0.105 mL of 0.05 M $Er(NO_3)_3$ were added to a aqueous solution (2 mL) containing different amounts of $Na_2HPO_4 \cdot 12H_2O$. Under ultrasonication, 0.2925 g EDTA was added to the solution and the pH of the mixture was adjusted to 8.5 with HNO_3 or NaOH. Then, 10 mL glycol and 0.0675 g CTAB were added to the solution. After the solution became clear, another aqueous solution containing 0.5 mL HF was dropwise added to the mixture and adjusted the pH to 2. After vigorous stirring at room temperature for 30 min, the colloidal solution were transferred into a 50 mL Teflon-lined autoclave, sealed and maintained at 180 °C for 1 - 12 h. The systems were then allowed to naturally cool to room temperature. The final products were collected by means of centrifugation, washed with ethanol and deionized water for several times to remove any possible remnants, and then dried in vacuum at 70 °C to obtain the dried UCNCs powder.

3 Results and Discussion

3.1 The rapid transformation of $NaYF_4$: Yb^{3+},Er^{3+} nanocrystals from cubic to hexagonal

It has been reported that $NaYF_4$:Yb^{3+},Er^{3+} nanocrystals can be obtained using hydro/solvothermal method with EDTA and CTAB as additives for controlling the size and prevent the nanocrystals from aggregating and the formation of pure β-$NaYF_4$:Yb^{3+},Er^{3+} nanocrystals should hydrothermal reaction 96 h.[10] However, It was found that the rapid crystal phase transformation of the $NaYF_4$:Yb^{3+},Er^{3+} nanocrystals from α- to β- phase can carry out in the presence of $Na_2HPO_4 \cdot 12H_2O$. And the growth rate of $NaYF_4$:Yb^{3+},Er^{3+} nanocrystals can be controlled strictly by varying the molar ratio of phosphates to Ln^{3+} (Ln^{3+} represents the total amount of Y^{3+}, Yb^{3+} and Er^{3+}) in the aqueous model system. The XRD patterns in Fig. 1 of $NaYF_4$:Yb^{3+},Er^{3+} nanocrystals obtained at different molar ratios (0, 1, 2, 3 and 4) of $Na_2HPO_4 \cdot 12H_2O$ to Ln^{3+} show crystal structure evolution. When other parameters are kept unchanged and increase the concentration of $Na_2HPO_4 \cdot 12H_2O$, it can quickly promote the phase transformation from α- to β- phase. For example, in the absence of $Na_2HPO_4 \cdot 12H_2O$, only highly crystalline α- planes, such as (111), (200), (221) and (311) (JCPDS No. 77-2042) (α-$NaYF_4$:Yb^{3+},Er^{3+}) was presented at 180 °C for 3.5 h (Fig. 1 curve a). However, mixed-phase (α-

and β-) products are obtained when $Na_2HPO_4 \cdot 12H_2O$ is added. The relative peak strength of diffraction peaks of the (100), (110), (101), (111), (201) and (211) planes of standard β-$NaYF_4$:Yb^{3+},Er^{3+} structure gradually increase with the molar ratios of phosphates to Ln^{3+} from 1 to 3 (Fig. 1 curve b - d). The purity peaks of β- phase $NaYF_4$:Yb^{3+},Er^{3+} can be formed when the molar ratios increases to 4 (Fig. 1 curve e). The rapid transformation of crystal phase of $NaYF_4$:Yb^{3+}, Er^{3+} from α- to mixed phase and ultimately to β- phase with increase of $Na_2HPO_4 \cdot 12H_2O$ indicated that phosphate affect the crystal transformation in the hydrothermal process significantly.

The TEM characterization was performed to confirm the changes in morphology. As shown in Fig. 2, the $NaYF_4$:Yb^{3+},Er^{3+} nanocrystals with an average diameter of 24.5 nm (Fig. 2 A) which were prepared without phosphate were mainly composed of spherical nanocrystals. The HRTEM of this nanocrystals shows lattice distance of 0.28 nm which correspond to the d spacing of the (200) lattice planes of the α-$NaYF_4$:Yb^{3+},Er^{3+} structure (Fig. 2 B). A standard α- structure can be found from the diffraction rings in the selected area electron diffraction (SAED) pattern (Fig. 2 C) which can be assigned to the (111), (200), (221) and (311) planes, respectively. This findings demonstrate once again that the crystals obtained without phosphate have α- phase structures corresponding to the XRD patterns in Fig. 1 curve a. Although the

as-prepared $NaYF_4$:Yb^{3+},Er^{3+} with the mixed crystal phase prepared in the present of $Na_2HPO_4 \cdot 12H_2O$ still keep the mainly spherical morphology, the average diameter of these crystals increase to 30 nm when the molar ratios increase to 2 (as shown in Fig. 2 D). In addition, the lattice fringes show spaces of 0.314 nm (Fig. 2 E) which is matched well with the (111) lattice planes of the α-$NaYF_4$:Yb^{3+},Er^{3+} structure. Owing to the most particles remaining in α- phase, the diffraction rings in the SAED pattern (Fig. 2 F) remain the planes of standard α- phase planes and not easy to find β- phase planes. The morphology of $NaYF_4$:Yb^{3+},Er^{3+} nanocrystals obtained at 180 ^oC for 3.5 h with the molar ratio of $Na_2HPO_4 \cdot 12H_2O$ to Ln^{3+} is 4 has tended to become tetragonum as well as the average diameter of the crystals become to 70 nm (Fig. 2 G). The interplanar spacings of 0.30 nm and 0.286 nm correspond to d spacing values of the (100) and (101) planes of β-$NaYF_4$:Yb^{3+},Er^{3+} structure (Fig. 2 H). The diffraction rings of the SAED pattern shown in Fig. 2 I can be associated with the (100), (110), (101) and (201) planes of the standard β-$NaYF_4$:Yb^{3+},Er^{3+} structure. The results from TEM of $NaYF_4$:Yb^{3+},Er^{3+} nanocrystals obtained in the presence of phosphates was compared with that of XRD patterns in Fig. 1, showing good agreement with each other. These gives further evidence of the fast formation of β-$NaYF_4$:Yb^{3+},Er^{3+} nanocrystals with the assist of $Na_2HPO_4 \cdot 12H_2O$ in the reaction system. Based on the above analysis, we can conclude that the $Na_2HPO_4 \cdot 12H_2O$

has significant influence on the structures and shapes of the final products ($NaYF_4$:Yb^{3+},Er^{3+}) in this reaction system.

Temperature is another significant factor for controlling the crystallization of nanocrystals among the experimental variables.[30] The effect of hydrothermal reaction temperature on the phase of the $NaYF_4$:Yb^{3+},Er^{3+} nanocrystals was investigated and XRD patterns of the prepared particles was shown in Fig. S 1. The particles processed at different temperatures displayed distinctively different XRD patterns. The $NaYF_4$:Yb^{3+},Er^{3+} nanocrystal also exhibit mixed phase at 160 ^oC for 3 h when Na_2HPO_4/Ln^{3+} is 4. Moreover, with the increase of hydrothermal reaction temperature to reach 180 ^oC, the crystalline phase of the particles trend to β- phase with the intensities of the diffraction peaks of α- phase significantly decreased. When the temperature increased, pure β- phase can be obtained at 200 ^oC for 3 h with the same amount of Na_2HPO_4. When we further increased the Na_2HPO_4/Ln^{3+} molar ratio and reaction temperature, less time was needed to obtain β-$NaYF_4$:Yb^{3+},Er^{3+} nanocrystals. For example, the β-$NaYF_4$:Yb^{3+},Er^{3+} nanocrystals can be achieved at 200 ^oC for 2 h (Fig. S2). The synthesis conditions of pure β-phase are summarized in Table S1. However, with increasing in phosphate concentration in this reaction system, the $NaYF_4$:Yb^{3+},Er^{3+} with rod-like hexagonal phase was prepared (Fig. S 3), which agrees with the reported results.[7] In order to obtain the β-$NaYF_4$:Yb^{3+},Er^{3+}

nanocrystals with the perfect size and morphology, we chose Na_2HPO_4 to Ln^{3+} of 4 for further studying.

3.2 Possible growth mechanism of β-$NaYF_4$:Yb^{3+},Er^{3+} nanocrystals in the presence of phosphate.

We further investigated the influence of reaction time to $NaYF_4$:Yb^{3+},Er^{3+} nanocrystals in the assistance of Na_2HPO_4. It is well known that the growth profile of $NaYF_4$:Yb^{3+},Er^{3+} crystals is from amorphous form to α- phase and finally turn into the β- phase.[7, 30] To further verify the process of crystal growth, a series of XRD patterns of $NaYF_4$:Yb^{3+},Er^{3+} crystals by assistant of $Na_2HPO_4 \cdot 12H_2O$ (the Na_2HPO_4-to-Ln^{3+} molar ratio was 4 : 1) at 180 ^oC for different hydrothermal reaction time were collected and presented in Fig. 3 A. Only the diffraction peak of α-$NaYF_4$:Yb^{3+},Er^{3+} nanocrystals can be observed when the reaction time was 1 h (Fig. 3 A curve 1 h) and a new diffraction peak of β- phase of $NaYF_4$:Yb^{3+},Er^{3+} emerges for 2 h (Fig. 3 A curve 2 h). The fraction of the β- phase increased substantially when the time reached to 3 h, but α- phase was still present (Fig. 3 A curve 3 h). However, the α- phase disappeared completely, and pure β- phase can be successfully obtained at 180 ^oC for only 3.5 h (Fig. 3 A curve 3.5 h). The X-ray diffraction patterns of these crystals in Fig. 3 A match well with those calculated for α- phase (JCPDS No. 77-2042) and β- phase (JCPDS

No. 16-0334) $NaYF_4:Yb^{3+},Er^{3+}$. Apparently, the crystal formation in the presence of phosphate follow the process of α- phase to the mixed phase and ultimately to β- phase. As a comparison, the formation process of $NaYF_4:Yb^{3+},Er^{3+}$ crystals without the $Na_2HPO_4 \cdot 12H_2O$ in the reaction system was also investigated and the results are present in Fig. 3 B. Only diffraction peak of α- phase of $NaYF_4:Yb^{3+},Er^{3+}$ crystals can be observed at 180 ^oC for 3 h. The diffraction peak of β- phase of $NaYF_4:Yb^{3+},Er^{3+}$ crystals can only be found until the hydrothermal reaction time increased to 6 h (Fig. 3 B curve 6 h), and without obvious changes even though the reaction time increase to 12 h (Fig. 3 B curve 12 h). With reference to the test results, it has the similar crystals conformation process for $NaYF_4:Yb^{3+},Er^{3+}$ crystals whether $Na_2HPO_4 \cdot 12H_2O$ exists in the reaction system or not. That is to say, $Na_2HPO_4 \cdot 12H_2O$ has greatly accelerated the phase transitions process from α- to β- phase. Therefore, these facts also proved that the phosphate plays the more significant role in accelerating structure transition of $NaYF_4:Yb^{3+},Er^{3+}$ from α- to β- phase rather than changing the growth pattern of $NaYF_4:Yb^{3+},Er^{3+}$ crystals.

The morphologies of the $NaYF_4:Yb^{3+},Er^{3+}$ crystals by assistant of Na_2HPO_4 at 180 ^oC for different reaction time are investigated (Fig 4). Fig. 4 A shows some representative TEM images of the $NaYF_4:Yb^{3+},Er^{3+}$ nanocrystals prepared by assistant of $Na_2HPO_4 \bullet 12H_2O$ ($PO_4^{3-}/Ln^{3+} = 4$) when the reaction time was 1 h. All of these nanocrystals in Fig. 4 A are

highly uniform with spherical shapes and an average diameter of 22.4 nm which are similar to the nanocrystals obtained in the absence of phosphate. However, the particle sizes increased rapidly than the particles in Fig. 4 A with the increase of reaction time. It is clear that small crystals exists around the surface of the $NaYF_4:Yb^{3+},Er^{3+}$ crystals with lager sizes (Fig 4 B and C) by increasing the solvothermal time from 2 h to 3 h and the crystals become irregular. By increasing the time to 3.5 h, the small nanocrystals can be completely transformed into uniform nanocrystals with little changes on their size and morphology. The fairly uniform well-defined $NaYF_4:Yb^{3+},Er^{3+}$ nanocrystals with an average length of 70 nm was obtained after hydrothermal reaction 3.5 h (Fig 4 D). The corresponding particle size distribution histograms of $NaYF_4:Yb^{3+},Er^{3+}$ nanocrystals from different reaction time are shown in Fig. S 4. The results mentioned above demonstrated that the growth pattern of crystals in the presence of phosphate is similar to the formation processes of $NaYF_4:Yb^{3+},Er^{3+}$ nanocrystals in other reaction system and the size of it increases with time.[7] There are a few reports demonstrated that the morphology and crystal phase of $NaYF_4:Yb^{3+},Er^{3+}$ can be controlled via changing the fluoride sources and the F^-/Ln^{3+} molar ratio during the hydrothermal process[7, 8, 28, 31]. The small nuclei can be generated when the F^- ions in the solution to react with Ln^{3+} through strong coordination interaction. These nuclei can only grow into α-$NaYF_4:Yb^{3+},Er^{3+}$

nanocrystals in a very short reaction time, which is a high temperature metastable phase. When the reaction time is increased, the unstable α-$NaYF_4$:Yb^{3+},Er^{3+} nanocrystals trend to transform to β-$NaYF_4$:Yb^{3+},Er^{3+} nanocrystals (a thermodynamically stable phase) through a dissolution–renucleation process known as ostwald ripening.[32, 33] It is also reported that density of Ln^{3+} on the surfaces of hexagonal crystals larger than that of α- crystals. [34] Therefore, the excessive F^- more trend to combine with the Ln^{3+} of surface of hexagonal crystals, such as (100), (110), (101), (201) and (220), to decrease the average number of dangling bonds and chemical potential of this crystal plane and results in faster growth along this direction with anisotropic growth thus to promote the rapid transformation of crystalline from α- to β- phase.[7] The transform mechanism of $NaYF_4$:Yb^{3+},Er^{3+} in this work maybe it is the anions liking the F^- which play an important role in accelerating the rapid growth and transformation of the nuclei of $NaYF_4$:Yb^{3+},Er^{3+}. A possible phase and morphology evolution mechanism in this paper is shown in Fig. 5. The abundant phosphate anions interact with the cations (Ln^{3+}) on the surface of β- crystal during the reaction and results in faster growth along this direction. It is means that negative ions can be absorbed to the growing nanocrystals' surfaces via physical and chemical bonding to prompt the formation of a uniform β- phase of $NaYF_4$:Yb^{3+},Er^{3+}. To confirm this assume, different sodium salts with the same concentration of Na^+ (the

Na^+-to-Ln^{3+} molar ratio was 8) were investigated to explore the influence on the crystal structure of $NaYF_4$:Yb^{3+},Er^{3+} nanocrystals at 180 ^oC for 3 h. Compared to the blank sample without any sodium salts system (Fig. 6 curve a), the XRD pattern of $NaYF_4$:Yb^{3+},Er^{3+} in NaCl system (Fig. 6 curve b) and Na_2SO_4 system (Fig. 6 curve c) clearly show that these sodium salts can also contribute to the transformation of crystals from α- to β- phase but with different effects. The intensities of the diffraction peaks of β- shapes also increase significantly when $(NH_4)_2HPO_4$ (Fig. 6 curve e) was used to replace Na_2HPO_4 (Fig. 6 curve d) in the same condition. The slight differences of $(NH_4)_2HPO_4$ and Na_2HPO_4 with the same concentration of PO_4^{3-} to the transition from α- to β- phase may attribute to the NH_4^+ which may affect the pressure of the reaction system. These results demonstrated that the influence on the transformation of $NaYF_4$:Yb^{3+},Er^{3+} nanocrystal originated in anion rather than sodium ions. Thus, compared to Cl^- and SO_4^{2-}, the phosphate anions with the most obvious effect to promote the rapid transformation of $NaYF_4$:Yb^{3+},Er^{3+} nanocrystals from α- to β- phase may owe to the strongest complexation of phosphate anions to Ln^{3+}.[35]

3.3 Upconversion fluorescence properties

The upconversion fluorescence of $NaYF_4$:Yb^{3+},Er^{3+} nanocrystals synthesized with different PO_4^{3-}/Ln^{3+} ratios (0 - 4) has been studied and

its upconversion fluorescence spectrum with different phase compositions and sizes are shown in Fig. 7 A. The fluorescence spectrum of UCNCs reveals typical emission bands at 535 nm, 550 nm and 660 nm under NIR excitation (980 nm), which can be assigned to the $^4H_{11/2} \rightarrow {}^4I_{15/2}$, $^4S_{3/2} \rightarrow {}^4I_{15/2}$ and $^4F_{9/2} \rightarrow {}^4I_{15/2}$ transitions of the Er^{3+} ions, respectively (Fig S. 5). Keeping all the other experimental measurements conditions (e.g., excitation source, excitation intensity and concentration) unchanged, the green upconversion fluorescence intensity at 550 nm (Fig. 7 A) and 660 nm (inset of Fig.7 A) of $NaYF_4:Yb^{3+},Er^{3+}$ nanocrystals increase with the ratios of PO_4^{3-} to Ln^{3+} from 0 to 4. Fig. 7 B is the fluorescence intensity ratios of integral intensity of green (550 nm) and red (660 nm) emission of the crystals with different phase. It is clear that the fluorescence intensity of pure β-$NaYF_4:Yb^{3+},Er^{3+}$ nanocrystals is about 22.5 times at 550 nm and 12.9 times at 660 nm higher than those of pure α-$NaYF_4:Yb^{3+},Er^{3+}$, respectively (Fig.7 B). The fluorescence brightness of $NaYF_4:Yb^{3+},Er^{3+}$ nanocrystals with different phase compositions, i.e., pure α- phase, α/β mixed phase, and pure β- phase, distinct from each other excited with a 980 nm CW laser (inset of Fig. 7 B). As known to all that the phase, morphologies and particle size of $NaYF_4:Yb^{3+},Er^{3+}$ nanocrystal attributed to the upconversion fluorescence intensities.[9] β-$NaYF_4:Yb^{3+},Er^{3+}$ nanocrystal has much higher fluorescence efficiency

than that of α-$NaYF_4$:Yb^{3+},Er^{3+}[7, 8] and the crystals with larger size result in lower surface defects and stronger emission.[9] The $NaYF_4$:Yb^{3+},Er^{3+} nanocrystals prepared in this paper have larger sizes and hexagonal phase. Based on this fact, the enhanced fluorescence may be caused by the different particle size and phase. It was also suggested that the upconversion fluorescence efficiency of $NaYF_4$:Yb^{3+},Er^{3+} nanocrystals depend on its structure and crystal growth characterization.

4 Conclusion

In summary, the β-$NaYF_4$:Yb^{3+},Er^{3+} nanocrystals have been successfully achieved using a simple and manageable hydrothermal method by assist of phosphate and templates and catalysts free. Through the simple manipulation of the phosphate to Ln^{3+} ratio, the nanocrystals with different structure and sizes can be prepared. The high purity β-phase crystal can be obtained at relatively low temperatures (180 ^{o}C) and in a very short period of time (< 3.5 h). And then, The β-$NaYF_4$:Yb^{3+},Er^{3+} nanocrystals synthesized here with small sizes (70 nm) and spherical morphology are expected to meet the requirements of biological applications. This synthetic strategy by adjusting the amount of inorganic salts and other reaction parameters can also be extended to the controllable synthesis of other inorganic compounds.

Acknowledgments

This work was supported by the National Natural Science Foundation of China (21375037, 21275051), Scientific Research Fund of Hunan Provincial Education Department (12A084), Science and Technology Departments (13JJ2020), and Doctoral Fund of Ministry of Education of China (20134306110006).

References:

1. L. Levy, Y. Sahoo, K.-S. Kim, E. J. Bergey and P. N. Prasad, *Chem. Mater.*, 2002, **14**, 3715-3721.
2. Y. Yi, G. Zhu, C. Liu, Y. Huang, Y. Zhang, H. Li, J. Zhao and S. Yao, *Anal. Chem.*, 2013, **85**, 11464-11470.
3. B. Yin, J. Deng, X. Peng, Q. Long, J. Zhao, Q. Lu, Q. Chen, H. Li, H. Tang, Y. Zhang and S. Yao, *Analyst*, 2013, **138**, 6551-6557.
4. F. Lin, B. Yin, C. li, J. Deng, X. Fan, Y. Yi, C. Liu, H. Li, Y. Zhang and S. Yao, *Anal. Methods*, 2013, **5**, 699-704.
5. G. Yi, H. Lu, S. Zhao, Y. Ge, W. Yang, D. Chen and L.-H. Guo, *Nano Lett.*, 2004, **4**, 2191-2196.
6. S. Huang, D. Wang, C. Li, L. Wang, X. Zhang, Y. Wan and P. Yang, *CrystEngComm*, 2012, **14**, 2235-2244.
7. Y. Wang, R. Cai and Z. Liu, *CrystEngComm*, 2011, **13**, 1772-1774.
8. M. Ding, C. Lu, L. Cao, Y. Ni and Z. Xu, *CrystEngComm*, 2013, **15**, 8366-8373.
9. M. Lin, Y. Zhao, M. Liu, M. Qiu, Y. Dong, Z. Duan, Y. H. Li, B. Pingguan-Murphy, T. J. Lu and F. Xu, *J. Mater. Chem. C*, 2014, **2**, 3671-3676.
10. L. Wang, R. Yan, Z. Huo, L. Wang, J. Zeng, J. Bao, X. Wang, Q. Peng and Y. Li, *Angew. Chem. Int. Ed.*, 2005, **44**, 6054-6057.
11. J. Liu, H. Luo, P. Liu, L. Han, X. Zheng, B. Xu and X. Yu, *Dalton Trans.*, 2012, **41**, 13984-13988.
12. D.-K. Ma, S.-M. Huang, Y.-Y. Yu, Y.-F. Xu and Y.-Q. Dong, *J. Phy. Chem. C*, 2009, **113**, 8136-8142.
13. H. W. Hugosson, O. Eriksson, U. Jansson, A. V. Ruban, P. Souvatzis and I. A. Abrikosov, *Surf. Sci.*, 2004, **557**, 243-254.
14. P. Broqvist, H. Grönbeck and I. Panas, *Surf. Sci.*, 2004, **554**, 262-271.
15. R. Ryoo and S. Jun, *J. Phy. Chem. B*, 1997, **101**, 317-320.
16. J. Qi, H. Nan, D. Xu and Q. Cai, *Cryst. Growth Des.*, 2011, **11**, 910-915.
17. A. K. P. Mann, J. Fu, C. J. DeSantis and S. E. Skrabalak, *Chem. Mater.*, 2013, **25**, 1549-1555.
18. J. Niu, K. Harada, I. Nakatsugawa and T. Akiyama, *Ceram. Int.*, 2014, **40**, 1815-1820.
19. Y. Yang, Q. Shao, R. Deng, C. Wang, X. Teng, K. Cheng, Z. Cheng, L. Huang, Z. Liu, X. Liu and B. Xing, *Angew. Chem. Int. Ed.*, 2012, **51**, 3125-3129.
20. Y. Yang, F. Liu, X. Liu and B. Xing, *Nanoscale*, 2013, **5**, 231-238.
21. Y. Yang, B. Velmurugan, X. Liu and B. Xing, *Small*, 2013, **9**, 2937-2944.
22. A. D. Ostrowski, E. M. Chan, D. J. Gargas, E. M. Katz, G. Han, P. J. Schuck, D. J. Milliron and B. E. Cohen, *ACS Nano*, 2012, **6**, 2686-2692.
23. Q. Liu, Y. Sun, T. Yang, W. Feng, C. Li and F. Li, *J. Am. Chem. Soc.*, 2011, **133**, 17122-17125.
24. G.-S. Yi and G.-M. Chow, *Chem. Mater.*, 2006, **19**, 341-343.
25. F. Wang and X. Liu, *Chem. Soc. Rev.*, 2009, **38**, 976-989.
26. F. Wang and X. Liu, *J. Am. Chem. Soc.*, 2008, **130**, 5642-5643.
27. Zhuang, Liang, H. H. Y. Sung, Yang, Wu, I. D. Williams, Feng and Q. Su, *Inorg. Chem.*, 2007,

46, 5404-5410.

28. C. Li, J. Yang, Z. Quan, P. Yang, D. Kong and J. Lin, *Chem. Mater.*, 2007, **19**, 4933-4942.
29. F. Zhang, J. Li, J. Shan, L. Xu and D. Zhao, *Chem. Eur. J.*, 2009, **15**, 11010-11019.
30. F. Zhang, J. Li, J. Shan, L. Xu and D. Zhao, *Chem. Eur. J.*, 2009, **15**, 11010-11019.
31. C. Li, Z. Quan, P. Yang, S. Huang, H. Lian and J. Lin, *J. Phy. Chem. C*, 2008, **112**, 13395-13404.
32. N. J. J. Johnson, A. Korinek, C. Dong and F. C. J. M. van Veggel, *J. Am. Chem. Soc.*, 2012, **134**, 11068-11071.
33. C. Liu, Z. Gao, J. Zeng, Y. Hou, F. Fang, Y. Li, R. Qiao, L. Shen, H. Lei, W. Yang and M. Gao, *ACS Nano*, 2013, **7**, 7227-7240.
34. X. Liang, X. Wang, J. Zhuang, Q. Peng and Y. Li, *Adv. Funct. Mater.*, 2007, **17**, 2757-2765.
35. X. Liu and R. H. Byrne, *Geochim. Cosmochim. Acta*, 1997, **61**, 1625-1633.

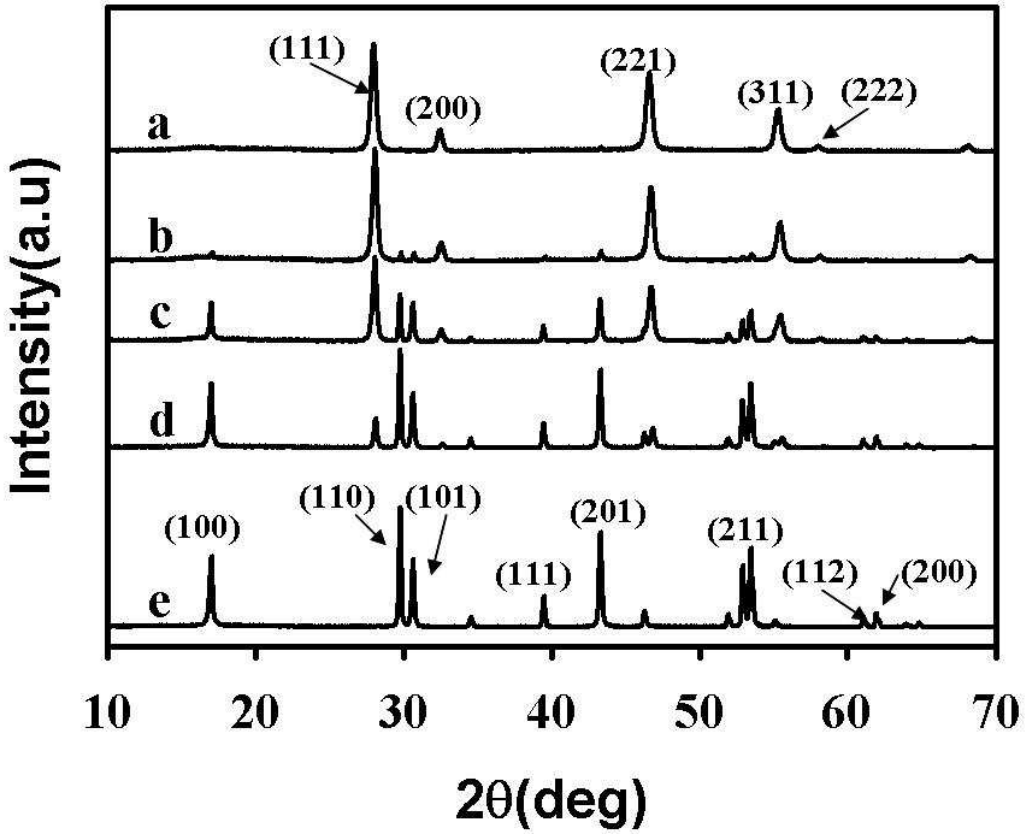

Fig.1 XRD pattern of α- to β- phase transformation of $NaYF_4:Yb^{3+},Er^{3+}$ nanocrystals with different mole ratio of phosphate to Ln^{3+}. The molar ratio of PO_4^{3-} to Ln^{3+} is a: 0, b: 1, c: 2, d: 3, e: 4 at 180 ^oC for 3.5 h. The standard data of α-$NaYF_4:Yb^{3+},Er^{3+}$ (black: JCPDS No. 77-2042) and β- $NaYF_4:Yb^{3+},Er^{3+}$ (red: JCPDS No. 16-0334) are given as references, respectively.

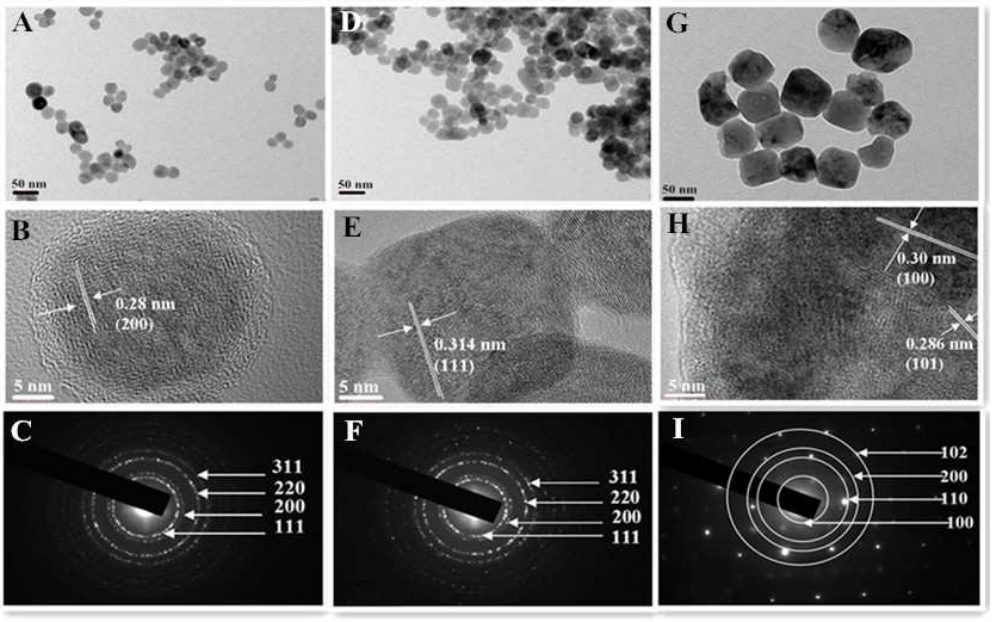

Fig.2 TEM , HRTEM and selected area electron diffraction (SAED) images of the synthesized $NaYF_4$:Yb^{3+},Er^{3+} crystal obtained at 180 ^oC for 3.5 h at different molar ratio of PO_4^{3-} to Ln^{3+}, *i.e.*, (A - C) 0, (D - F) 2, and (G - I) 4. The scale bars embedded in the TEM and HRTEM images correspond to 50 nm and 5 nm, respectively.

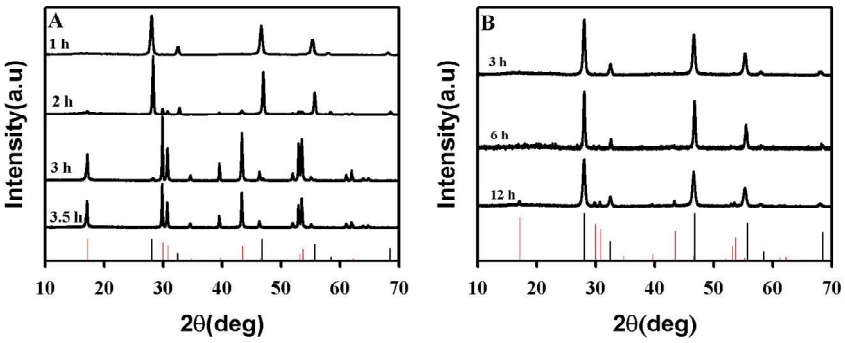

Fig. 3 The influence of hydrothermal time on the crystal structure of $NaYF_4:Yb^{3+},Er^{3+}$. XRD patterns of $NaYF_4:Yb^{3+},Er^{3+}$ (A) with the assistance of $Na_2HPO_4•12H_2O$ ($PO_4^{3-}/Ln^{3+} = 4$) and (B) without $Na_2HPO_4•12H_2O$. The products synthesized at 180 ^oC. The standard data of α-$NaYF_4:Yb^{3+},Er^{3+}$ (JCPDS No. 77-2042) and β-$NaYF_4:Yb^{3+},Er^{3+}$ (JCPDS No. 16-0334) are given as references, respectively.

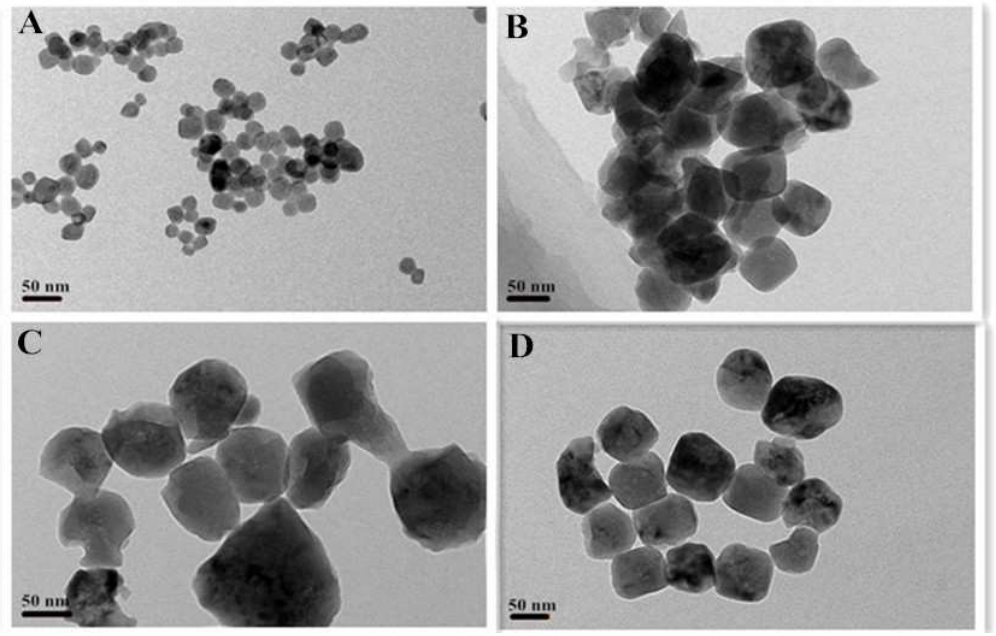

Fig. 4 TEM images of $NaYF_4:Yb^{3+},Er^{3+}$ crystals (PO_4^{3-} / Ln^{3+} = 4) prepared for different reaction time. (A) 1 h, (B) 2 h, (C) 3 h, (D) 3.5 h.

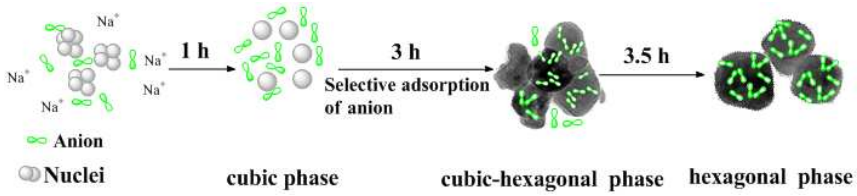

Fig. 5 Schematic diagram of crystal phase rapid transformation of $NaYF_4$,Yb^{3+},Er^{3+} nanocrystals with the assistance of salts.

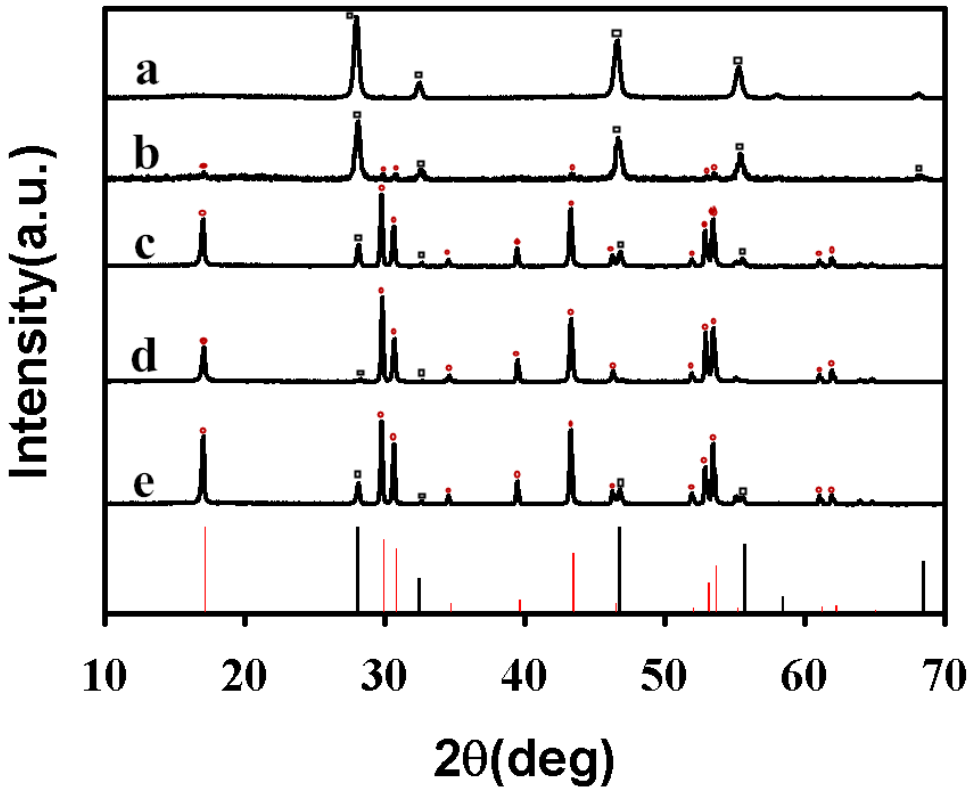

Fig.6 XRD patterns of $NaYF_4:Yb^{3+},Er^{3+}$ nanocrystals prepared in the assistance of different salts : (a) blank, (b) NaCl, (c) Na_2SO_4, (d) Na_2HPO_4, and (e) $(NH_4)_2HPO_4$. The molar ratio of Na^+ to Ln^{3+} is 8 for b, c and d, and PO_4^{3-} to Ln^{3+} is 4 for d and e. The pH was adjusted to 2 and keep at 180 ^oC for 4 h during the crystallization process. The standard data of α-$NaYF_4:Yb^{3+},Er^{3+}$ (JCPDS No. 77-2042) and β-$NaYF_4:Yb^{3+},Er^{3+}$ (JCPDS No. 16-0334) are given as references, respectively.

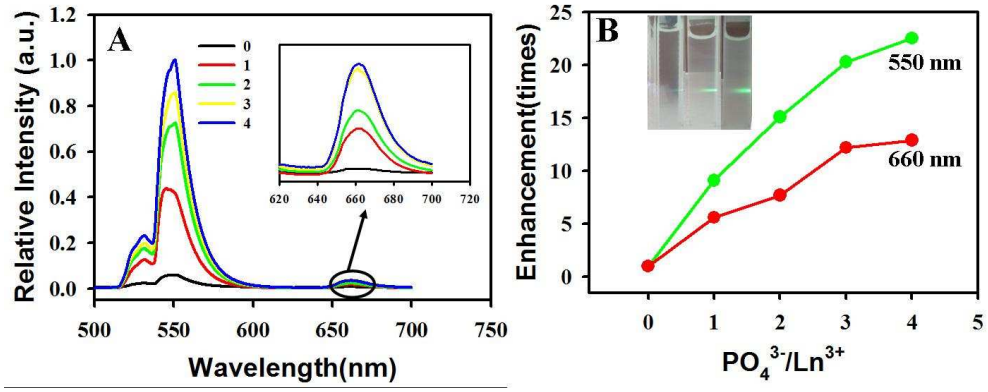

Fig. 7 (A) Upconvertsion fluorescence spectra of $NaYF_4:Yb^{3+},Er^{3+}$ nanocrystals synthesized with different PO_4^{3-}/Ln^{3+} ratios (0 - 4). Inset of A: the amplifying upconvertsion fluorescence spectra at 660 nm. (B) Enhancement times of the green (550 nm) and red (660 nm) emission of $NaYF_4:Yb^{3+},Er^{3+}$ nanocrystals synthesized with different PO_4^{3-}/Ln^{3+} ratios (0 - 4). Inset: the digital photograph of the samples with different PO_4^{3-}/Ln^{3+} ratios (from left to right) 0, 2 and 4, respectively.

Graphical Abstract

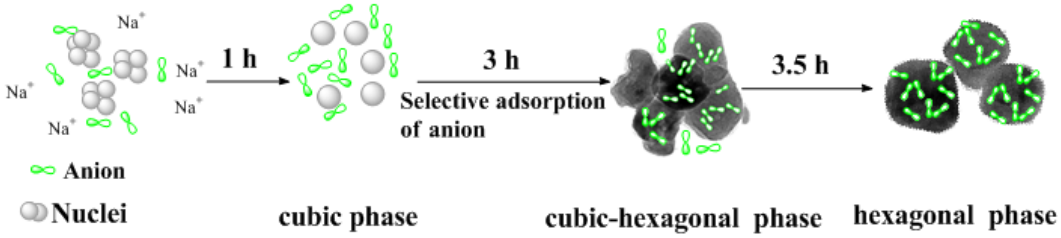

- High-quality hexagonal nanocrystals (β-$NaYF_4$:Yb^{3+},Er^{3+}) was obtained in aqueous solution via a facile hydrothermal route at relatively low temperature and in a short time.
- The size and structure of as-prepared $NaYF_4$:Yb^{3+},Er^{3+} can be controlled by changing the molar ratio of some salts to Ln^{3+} (Ln^{3+} represents the total amount of Y^{3+} and the doped rare earth elements such as Yb^{3+}, Er^{3+}), such as Na_2HPO_4.
- The β-$NaYF_4$:Yb^{3+},Er^{3+} nanocrystals with the relatively small size, spherical morphology and strong fluorescence are expected.
- This synthetic strategy by adjusting the amount of inorganic salts can also be extended to the controllable synthesis of other inorganic compounds.